Measurement Science and
Technology

PAPER • **OPEN ACCESS**

A mechanically stable laser diode speckle interferometer for surface contouring and displacement measurement

To cite this article: Daniel Francis *et al* 2015 *Meas. Sci. Technol.* **26** 055402

View the article online for updates and enhancements.

You may also like

- Experimental qualification by extensive evaluation of fibre optic strain sensors
Constanze Schilder, Nadine Kusche, Vivien G Schukar et al.
- Heterodyning of fibre optic electronic speckle pattern interferometers using laser diode wavelength modulation
H Atcha and R P Tatam
- Hooke's law experiment using an electronic speckle pattern interferometry
Jeongwoo Park and Jaehyuk Huh

This content was downloaded from IP address 202.8.112.197 on 06/07/2023 at 08:45

OPEN ACCESS
IOP Publishing
Measurement Science and Technology
Meas. Sci. Technol. **26** (2015) 055402 (7pp)
doi:10.1088/0957-0233/26/5/055402

A mechanically stable laser diode speckle interferometer for surface contouring and displacement measurement

Daniel Francis, Dackson Masiyano[1], Jane Hodgkinson and Ralph P Tatam

Engineering Photonics, Cranfield University, Cranfield, MK43 0AL, UK

E-mail: r.p.tatam@cranfield.ac.uk

Received 17 December 2014, revised 16 February 2015
Accepted for publication 27 February 2015
Published 9 April 2015

Abstract

Electronic speckle pattern interferometry (ESPI) is demonstrated using a simple configuration consisting of a wedged window and a beamsplitter. The window serves to produce a reference beam which is in-line with the scattered object beam. The system is almost common-path and therefore provides much better mechanical stability than conventional ESPI configurations, which have widely separated beam paths. The configuration has collinear observation and illumination directions and therefore has maximum sensitivity to out-of-plane displacement. Wavelength modulation through adjustment of the laser diode control current provides a convenient method of phase shifting without the need for external moving parts. Further, variation of the laser diode control temperature allows extended wavelength tuning to adjacent longitudinal modes, facilitating surface contouring measurements via the two-wavelength technique. The interferometer is demonstrated for surface displacement measurement with a 3.3 μm centre displacement measured over a 15 mm × 15 mm region of a flat plate. Contour measurements of a shaped object are made using an equivalent wavelength of 1.38 mm.

Keywords: ESPI, speckle, interferometry, contouring, laser diode

(Some figures may appear in colour only in the online journal)

1. Introduction

Speckle interferometry is a highly sensitive tool used for making full-field, non-contact measurements of surface properties at the micro-scale. It can be used to measure surface displacement [1, 2] and related parameters including displacement derivative [3], strain [4, 5], shape and slope [6, 7], curvature and twist [8], and vibration [9, 10]. Speckle interferometry is often subdivided into two distinct techniques: electronic speckle pattern interferometry (ESPI) [11], also known as digital speckle pattern interferometry (DSPI) and TV-holography, and speckle shearing interferometry, or shearography [12]. Both techniques have their own relative advantages and disadvantages, for instance, ESPI is directly sensitive to displacement, making it more suitable for shape and vibration measurements, whereas shearography is directly sensitive to displacement derivative, making it a better choice for strain measurement.

Another advantage of shearography, which has seen its widespread adoption in industrial non-destructive testing (NDT) to provide qualitative measurements, is its inherent resilience to environmental disturbances, including thermal drift, vibration, and rigid-body motion [13]. This is due to the optical configuration, which consists of, for instance,

[1] Now at Two Trees Photonics, Beaufort Court, 23 Roebuck Way, Knowlhill, Milton Keynes, MK5 8HL, UK.

Content from this work may be used under the terms of the Creative Commons Attribution 3.0 licence. Any further distribution of this work must maintain attribution to the author(s) and the title of the work, journal citation and DOI.

 © 2015 IOP Publishing Ltd Printed in the UK

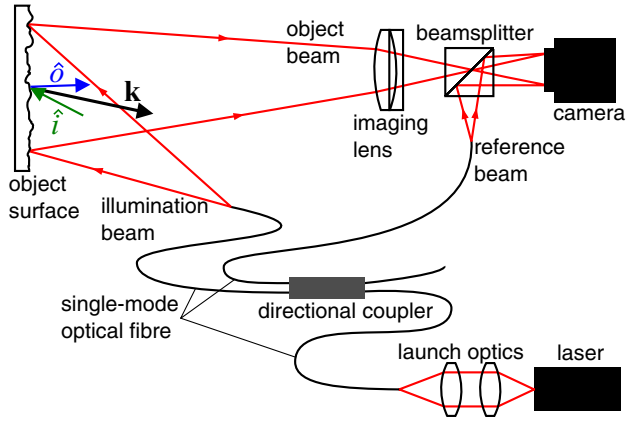

Figure 1. Schematic showing a typical optical arrangement for ESPI using a fibre-optic directional coupler to produce illumination and reference beams. This configuration highlights the large difference in the optical paths of the two arms of the interferometer which contributes to the technique's susceptibility to environmental disturbances. The sensitivity vector of the instrument (**k**), is indicated as the bisector of the observation ($\hat{o}$) and illumination ($\hat{i}$) vectors.

a Michelson interferometer [14], prism [15], or diffractive element [16], each of which have only a small separation of optical beam paths before recombination. In contrast, the typical optical configuration for ESPI, such as that shown in figure 1, has a very large separation of beams before recombination because, in this case, the illumination and object beams form part of the interferometer. Any environmental disturbances that affect one path relative to the other will result in phase variations within the interferometer. This will cause speckle decorrelation resulting in an increase in noise and a reduction in fringe visibility and in many practical applications complete decorrelation and loss of signal. In figure 1, the laser light is divided into illumination and reference beams using the fibre-optic coupler, typically with a split ratio of 95:5 object beam/reference beam power. Light illuminating the object's surface forms a speckle pattern which is imaged by the camera. The beamsplitter located in front of the camera serves to combine light in the reference arm with the scattered light (object beam) producing an interferometric speckle pattern which is sensitive to displacement in the direction given by the bisector of the illumination ($\hat{i}$) and observation ($\hat{o}$) beam vectors (the sensitivity vector), which in this case is predominantly out-of-plane.

A number of researchers have published work describing ESPI with improved mechanical stability and resilience to disturbance. One method, that was used to determine displacements associated with residual stresses, involves using modified shearography [17]. If shearography is set up so that the image shear is large enough such that one of the images is obtained from a region of the surface that experiences no displacement during deformation, then the speckle pattern is purely sensitive to displacement, and the results are equivalent to ESPI. Such systems are very stable mechanically, however the fringe patterns are noisier than conventional ESPI due to the combination of two speckle patterns as opposed to a speckle pattern and smooth reference wave.

In another design, presented by Hansen [18], the scattered object beam is viewed through a glass plate from which a reference is taken by reflection from the front surface. With this device, the only separation of the interfering beam paths is in the gap between the object surface and the glass plate, which can be as small as a centimetre or so. Phase analysis is performed using temporal phase stepping [19] implemented by mounting the glass plate on a piezo-electric transducer. This interferometer has a similar design to that of Peng *et al* [20] who developed a compact system which used a specular reflection from a glass plate as a reference wave. The interferometer also used phase stepping implemented through mechanical means by mounting the glass plate on a piezo-electric transducer.

The system presented here works on a similar principle to that of [18] and [20], in that it utilizes the Fresnel reflection from a window placed in the path of the illumination beam to produce a reference beam. However, in our approach no mechanical phase stepping is required. The system is used with a semiconductor laser diode which is held at a fixed wavelength using temperature and current controllers. Modulation of the control current and/or temperature results in a variation in the output wavelength. This causes a change of phase in the interferometer $\Delta\phi$, which is dependent on the pathlength imbalance Δl (twice the separation between the object and the window) and is given by [21, 22]

$$\Delta\phi = \frac{2\pi}{c}\Delta\nu\Delta l \tag{1}$$

where $\Delta\nu$ is the change in optical frequency and c is the free-space speed of light. This property allows phase demodulation using temporal phase stepping to be applied on the laser itself, without the need for any external moving components provided the wavelength change required is within a mode-hop free region of the diode. Further tuning so that the output switches to an adjacent longitudinal mode allows surface contouring measurements to be made using the two-wavelength technique [23]. Contour measurements made with this system are presented in section 4. Another difference with the system described here relative to those of [18] and [20] is the orientation of the observation and illumination directions, which are collinear. This allows for maximum out-of-plane sensitivity with zero contribution from in-plane components.

2. Reference window speckle interferometer

The optical layout of the reference window speckle interferometer is shown in figure 2. The design concept for the interferometer arose from our work investigating diffuse reflections in tunable diode laser spectroscopy [24]. The laser diode was an SDL-5431-G1 mounted in a Profile LDH CDTC B driver and has maximum power of 100 mW and centre wavelength of 832 nm. The diode current and temperature were stabilized using a Profile LDC 200 and a Thorlabs TED 200 respectively. The output of the laser was collimated using a 100 mm focal length lens after which it was incident on a pellicle beamsplitter at which 50% was dumped and 50% transmitted towards the object. Light scattered from the object was imaged via the beamsplitter onto the camera. The camera used was a

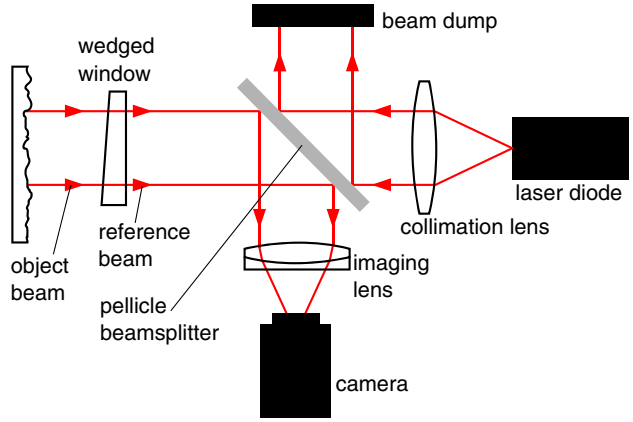

Figure 2. Schematic showing the reference window speckle interferometer. The wedged window is used to obtain a smooth reference wave.

Baumer HXC-13 CMOS camera with 1024 × 1280 pixels that are each 14 μm × 14 μm. The large pixels ensure that the sensor provides excellent sensitivity and dynamic range (ISO2500, 90 dB) at the cost of potentially reduced spatial resolution. The camera is capable of 500 frames per second at full frame and faster speeds are achievable using reduced interrogation regions. Data from the camera was acquired using an NI-PCI-1433 frame grabber housed in a PC running LabVIEW TM.

The reference beam is obtained from the Fresnel reflection from the surface normal to the optical axis of the wedged window placed in the beam path 2.5 cm away from the object's surface. The choice of a wedged window as opposed to a window with two parallel surfaces was made in order to minimize the influence of interference effects that may be caused due to reflections from the window surfaces. The angle of the wedged surface was 5°. The ratio of speckle pattern to reference beam intensities can be optimised using anti-reflection coatings on the surface of the window. For maximum energy efficiency and field of view, the collimated beam diameter should be matched to the aperture diameter of the reference window. The distance between the window and the object surface was chosen to minimize the separation of optical paths between the object and reference beams whilst ensuring that the required wavelength shift needed to obtain all necessary phase stepped images was within a mode-hop free tuning region of the laser, according to equation (1).

The field of view is limited by the dimensions of the window and its mount and has a clear aperture of approximately 23 mm diameter. Larger fields of view can be achieved by using larger windows however this would require larger area collimated beams which would reduce the energy density of the incident light for a source of a given power, resulting in reduced fringe contrast. To image the surface so that a large region of the camera's sensor was illuminated, thus ensuring images with a high spatial resolution, a 1.25 × imaging microscope objective was used. This was used in conjunction with a 180 mm focal length lens that decreased the working distance and reduced the field of view compared with using the objective alone. A photograph showing the aligned interferometer with the imaging optics is shown in figure 3.

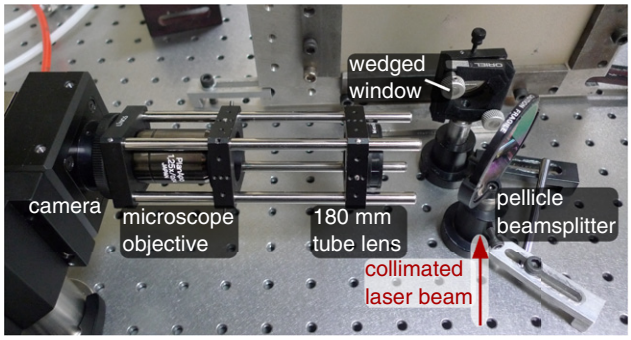

Figure 3. Photograph showing interferometer alignment and imaging optics.

3. Measurement of surface displacement

The interference between the speckled wavefront produced by scattered light from the object's surface and the smooth reference wave obtained from reflection from the window produces an interferometric speckle pattern which is imaged by the camera. Any subsequent displacement of the object's surface causes a change in the intensity of the speckles within the pattern, which cycle from dark to light to dark again as the phase change due to the deformation varies by 2π. Fringes contouring the magnitude of the displacement can be generated by correlating interferometric speckle patterns recorded before and after deformation, commonly by digital subtraction and rectification. The relative displacement between points in the image coinciding with consecutive fringe minima (or maxima) is equal to half the wavelength of the illuminating light. The component of displacement that the interferometer is sensitive to is determined by the sensitivity vector

$$\mathbf{k} = \hat{o} - \hat{i} \tag{2}$$

where $\hat{o}$ and $\hat{i}$ are unit vectors in the observation and illumination directions respectively. For the interferometer described here, the observation and illumination directions are collinear.

A typical correlation fringe pattern, obtained in response to a point displacement in the centre of a perimeter clamped flat aluminium plate imparted by a micrometer screw, is shown in figure 4(*a*). The field of view is approximately 15 mm × 15 mm and this is limited by the aperture of the wedged window as discussed previously.

Calculation of the displacement induced phase change in the interferometer was achieved using temporal phase stepping, implemented by wavelength modulation via adjustment of the laser diode control current. The current controller was activated externally using a NI 9263 analogue output module in a NI cDAQ-9174 data acquisition chassis. The five-step algorithm [25] was chosen for phase calculation which involves recording a series of five images with a relative phase difference of π/2. The optical frequency shift required to produce a π/2 phase shift with a 5 cm pathlength imbalance is 1.5 GHz, from equation (1). The change in control current required to achieve this was calibrated by recording an initial image and then incrementing the current. Subsequent recorded images were subtracted from the initial image and a 2π phase shift was determined when the mean intensity of the subtracted

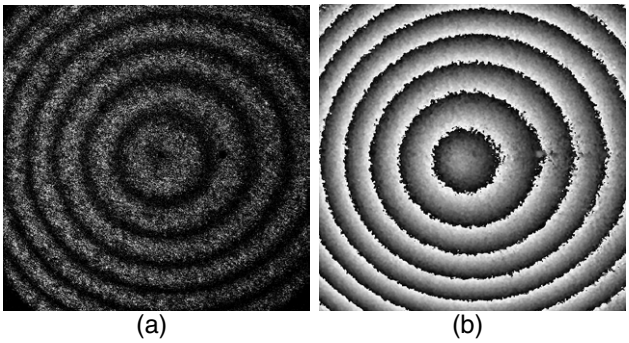

Figure 4. (*a*) Correlation fringe pattern obtained with the reference window speckle interferometer as a response to a point displacement in the centre of a flat plate. (*b*) Wrapped phase map obtained using temporal phase stepping through laser diode current modulation. The field of view of the images is 15 mm × 15 mm.

image reached a minimum [21]. The algorithm is applied to the series of images recorded both before and after deformation and the phase of each is calculated using the equation

$$\phi = \tan^{-1}\left[\frac{2(I_2 - I_4)}{2I_3 - I_5 - I_1}\right] \tag{3}$$

where $I_{1\text{–}5}$ are the intensities of the five phase stepped images. This algorithm was chosen due to its ability to compensate for calibration errors [25]. The phase difference associated with the displacement was obtained by subtracting the phases calculated before (ϕ_I) and after (ϕ_F) deformation using [26]

$$\Delta\phi = \begin{cases} \phi_F - \phi_I & \text{for } \phi_F \geq \phi_I \\ \phi_F - \phi_I + 2\pi & \text{for } \phi_F < \phi_I \end{cases} \tag{4}$$

The calculated phase was wrapped in the region of 0 to 2π producing the fringe discontinuities seen in the wrapped phase map, such as that shown in figure 4(*b*). The wrapped phase map was processed with an iterative sine-cosine filter [27] to reduce high frequency noise associated with speckle decorrelation. In order to make quantitative measurements, the phase fringe discontinuities need to be removed by phase unwrapping. This was done using the 2D iso-phase unwrapper [28] which was developed by researchers at Liverpool John Moores University who have open source C++ implementations available on their website [29]. The out-of-plane displacement w is related to the phase change $\Delta\phi$ by

$$w = \frac{\Delta\phi \cdot \lambda}{4\pi} \tag{5}$$

where λ is the wavelength [11]. The unwrapped phase calculated from the image shown in figure 4(*b*) is shown in figure 5(*a*) and the out-of-plane displacement calculated from this data is shown in figure 5(*b*).

4. Surface contouring using the two-wavelength technique

ESPI can be used to measure the surface height profile of non-planar objects. The fringes that are generated are dependent on the difference in the surface profile from the image plane and correspond to regions of equal height from this plane,

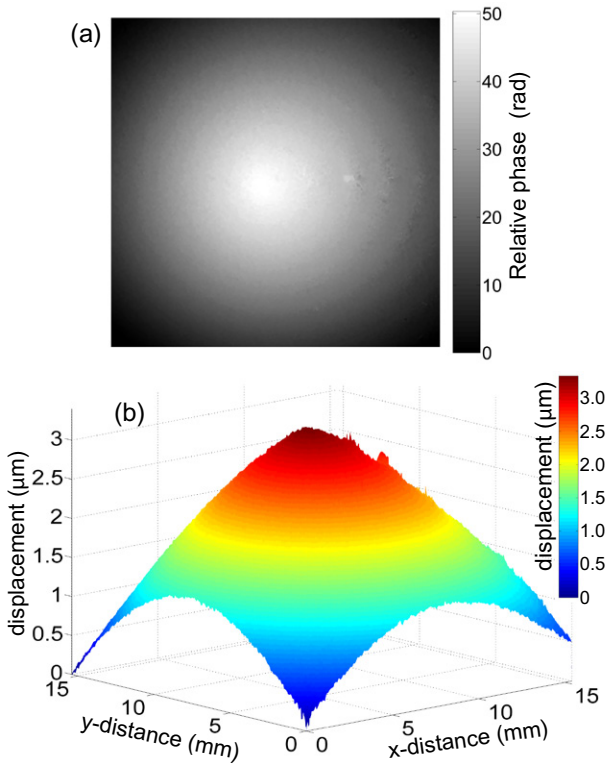

Figure 5. (*a*) Unwrapped phase map and (*b*) the calculated displacement across the image.

like the contours on a map. The separation of these contour fringes is equal to $\lambda/2$ if the instrument is sensitive to only the out-of-plane component, which, when using visible monochromatic sources is too small for practical use. To overcome this limitation the two-wavelength technique was developed, which involves correlating images recorded at two distinct wavelengths λ_1 and λ_2 [23]. This results in a fringe pattern equivalent to that that would be obtained if a potentially much longer equivalent wavelength Λ were used, given by

$$\Lambda = \frac{\lambda_1\lambda_2}{|\lambda_1 - \lambda_2|} \tag{6}$$

The separation of the contour fringes is then dependent on the separation of the two constituent wavelengths with smaller wavelength separations giving larger equivalent wavelengths. The surface height z can be determined quantitatively from the phase difference $\Delta\phi$ of images recorded at the two wavelengths using the equation

$$z = \frac{\Delta\phi}{2\pi \cdot k_z} \cdot \Lambda \tag{7}$$

where the sensitivity vector $\mathbf{k} = (k_x, k_y, k_z) = (0, 0, 2)$ for our setup with collinear observation and illumination vectors.

One of the issues with combining dual-wavelength shape measurement with phase shifting interferometry is that the phase step calibration for one wavelength will not be the same for the other wavelength. Uncertainties in the phase measurement will therefore be introduced if the same phase step is used for both wavelengths. This uncertainty is reduced when higher order, error compensating phase stepping algorithms

Figure 6. Light bulb coated with reflective paint that was used to demonstrate the interferometer's surface contouring ability.

are used. Schmit and Hariharan [30] presented an eight-step algorithm which yields almost perfect compensation when compared to lower order algorithms. They showed that while the five-step algorithm (equation (3)) shows good compensation, with errors less than $5 \times 10^{-4}\lambda$ for up to 3 degrees of miscalibration, the phase errors associated with their eight-step algorithm are less than 5×10^{-5} of a wavelength up to 20 degrees of miscalibration. Their eight-step algorithm is given by

$$\phi = \tan^{-1}\left[\frac{5I_2 - 15I_4 + 11I_6 - I_8}{I_1 - 11I_3 + 15I_5 - 5I_7}\right] \tag{8}$$

where $I_{1\text{–}8}$ are the intensities of the eight phase stepped images. These higher order phase stepping algorithms have been used before in speckle interferometric surface profiling measurements. Kumar *et al* used seven-step [31] and eight-step algorithms [32] for micro-scale shape measurements. Measurements at this scale need relatively small equivalent wavelengths, which can be achieved using relatively widely spaced constituent wavelengths. For instance, in [31] the He:Ne and Nd:YAG wavelengths, 632.8 nm and 532 nm respectively were used which gives an equivalent wavelength of 3.34 mm, and in [32] additionally a He:Cd laser (441.6 nm) was used which in combination with the former wavelengths provides a range of equivalent wavelengths from 1.46 μm to 11.74 μm.

The surface contouring capability of the reference window speckle interferometer was demonstrated on a small light bulb that was 21 mm long and 11 mm wide across the bulb. This object was chosen for its surface height variation and its dimensions which allowed it to be placed within the field of view of the instrument. The light bulb was coated with a reflective paint to ensure that a speckle pattern was produced when illuminated by the collimated laser beam. A photograph of the painted light bulb is shown in figure 6. The use of flash highlights the reflective nature of the paint.

To produce the two wavelengths necessary to generate a suitable equivalent wavelength, the laser diode control temperature

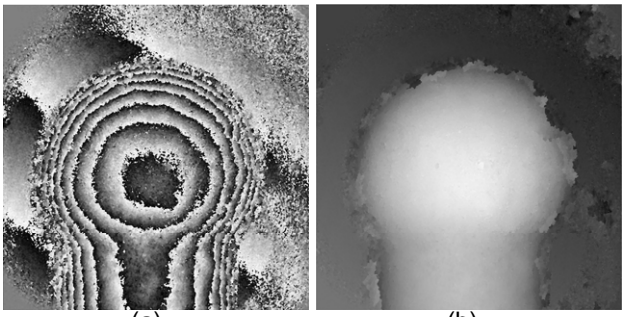

Figure 7. (*a*) Wrapped and (*b*) unwrapped phase maps of a light bulb generated using an equivalent wavelength of 1.38 mm.

was modulated so that the output tuned to an adjacent longitudinal mode. Figure 7 shows wrapped and unwrapped phase maps that were produced from phase measurements made with the control temperature set at 15 °C and 18 °C. The wavelength versus control temperature properties were measured using an optical spectrum analyser (Advantest Q8381) and were found to be 831.3 nm ± 0.03 nm and 831.8 nm ± 0.03 nm at control temperatures of 15 °C and 18 °C respectively. The uncertainty in the wavelength measurements (±0.03 nm) was taken from the standard deviation of twenty measurements made at a fixed wavelength. The spectrum analyser has an accuracy of 0.5 nm, however any systematic error would be the same for both measurements and will cancel in the subtraction in equation (6). This results in an equivalent wavelength of Λ = 1.38 mm ± 0.12 mm, where the uncertainty was calculated from the combination of the errors given above. The phase stepping was performed using the approach discussed previously at each wavelength using the eight-step algorithm. The phase step used is only correct for a locus of points of equal height on the object. Using equation (1) with a pathlength imbalance Δl of 5 cm, the phase error is calculated to be 0.01 π (1.8°) per millimetre of pathlength variation due to object height. This error is well compensated for using the eight-step algorithm given the miscalibration figures quoted previously and the limiting factor is the uncertainty on the wavelength measurements. The surface height profile calculated from the unwrapped phase map in figure 7(*b*) using equation (7) is shown in figure 8.

The total measured height variation across the bulb is 3.39 mm ± 0.29 mm. The uncertainty in the height measurement was obtained from the uncertainty in the wavelength measurements, since this was the main source of error. The total height of the bulb cannot be measured because the step change in height from the bulb to the background upon which it is mounted is too large for this equivalent wavelength. Also, the height variation increases rapidly at the edges of bulb as can be seen by the noisy, high spatial frequency fringes around the periphery of the bulb in figure 7(*a*) and data in these regions is filtered out as noise. A comparison with mechanical measurement can be made from the difference in height from the stem of the bulb and the head of the bulb. The mean height difference between the head and the stem of the bulb from figure 8 is 1.10 mm. The height difference between the head and the stem of the bulb measured with a set of Vernier callipers is 1.05 mm, which is within the measurement uncertainty.

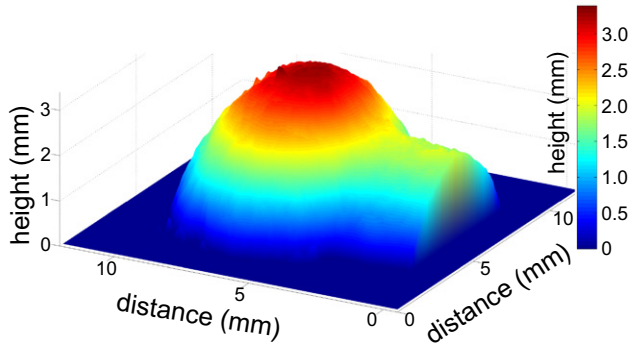

Figure 8. Surface height profile of a light bulb calculated from the unwrapped phase map shown in figure 7(*b*).

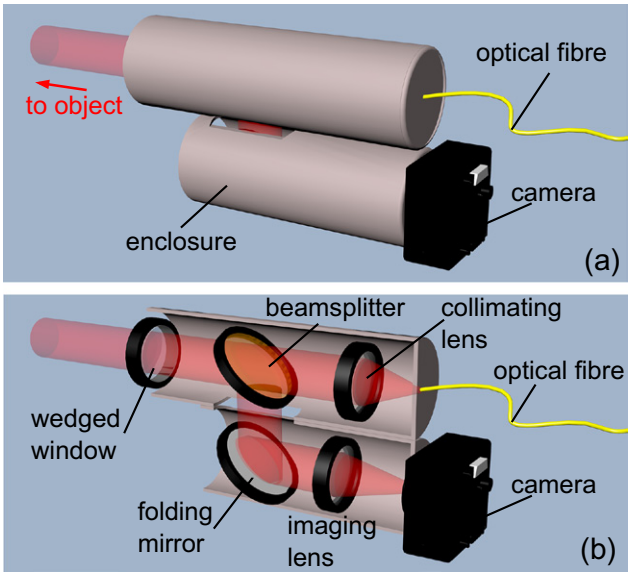

Figure 9. A concept design for a portable speckle interferometer based on the reference window arrangement shown (*a*) enclosed and (*b*) in cross section revealing the optical components.

5. Discussion and conclusions

The in-line reference window interferometer presented here has been demonstrated to measure static out-of-plane surface displacements and surface height profiles. The simple optical design, utilizing the reflection from a wedged window in the beam path to produce a smooth reference wave ensures a small separation of paths between the interfering beams resulting in highly stable fringes. Interferometric processing by modulating the control parameters of the laser diode enables quantitative measurements to be made with no external moving parts. The configuration, featuring collinear observation and illumination directions is maximally sensitive to the out-of-plane component of displacement, with zero contribution from the in-plane components.

The design could even potentially allow for the development of a portable instrument. Figure 9 shows a concept design for such an instrument based on the optical arrangement of figure 2 with a few modifications. In this design, beam delivery is provided by a single-mode optical fibre which allows the laser diode and its required control electronics to be located remotely from the device. The folding mirror makes the system more compact and additionally further imaging optics could be placed between the window and the beamsplitter to improve the field of view. A handheld system could possibly be envisaged if the image acquisition was sufficiently fast that the associated timescales were short compared with any mechanical perturbations.

In order for a handheld system to work, the total measurement time would need to be less than 0.1 s. If we assume that the time taken for wavelength tuning is much less than the image acquisition time then the total measurement time is equal to the time required to capture all images required to produce a wrapped phase map. This would require a camera capable of at least 100 frames per second for the five-step algorithm or 160 frames per second for the eight-step algorithm, whilst capturing sufficient light within an exposure time of 10 ms and 6.25 ms for the two algorithms respectively. This is achievable using commercially available cameras including the one used here. The range of stand-off distances over which the instrument could be used is limited by the amount of scattered light available and the coherence length of the laser. Also at larger distance the system is more susceptible to environmental disturbances, so would therefore work better for relatively close up measurements. The range of suitable object sizes is dependent on the available laser power and optics size, with larger objects requiring more laser power and larger optics.

We have demonstrated the interferometer for out-of-plane displacement measurement and surface contouring using a flat aluminium plate for the former and a painted light bulb for the latter. A displacement magnitude of 3.3 μm was observed across the 15 mm × 15 mm field of view for the measurement shown. A surface height variation of 3.39 mm was measured across the light bulb using an equivalent wavelength of 1.38 mm.

Acknowledgments

We could like to thank The Engineering and Physical Sciences Research Council (EPSRC), UK for supporting this work via grants EP/H02252X, GR/T04595 and GR/T04601. (For enquiries relating to access to the research data or other materials referred to in this article, please contact Cranfield University Library and Information Services—library@cranfield.ac.uk).

References

[1] Leendertz J A and Butters J N 1971 Speckle pattern and holographic techniques in engineering metrology *Opt. Laser Technol.* **3** 26–30
[2] Rastogi P K 2001 Surface displacements, derivatives and surface shapes *Digital Speckle Interferometry and Related Techniques* ed P K Rastogi (Chichester: Wiley)
[3] Leendertz J A and Butters J N 1973 An image-shearing speckle-pattern interferometer for measuring bending moments *J. Phys. E: Sci. Instrum.* **6** 1107–10
[4] Kästle R, Hack E and Sennhauser U 1999 Multiwavelength shearography for quantitative measurements of 2D strain distributions *Appl. Opt.* **38** 96–100

[5] Groves R M, Chehura E, Li W, Staines S E, James S W and Tatam R P 2007 Surface strain measurement: a comparison of speckle shearing interferometry and optical fibre Bragg gratings with resistance foil strain gauges *Meas. Sci. Technol.* **18** 1175–84
[6] Tatam R P, Davies J C, Buckberry C H and Jones J D C 1990 Holographic surface contouring using wavelength modulation of laser diodes *Opt. Laser Technol.* **22** 317–21
[7] Huang J-R, Ford H D and Tatam R P 1997 Slope measurement by two-wavelength electronic shearography *Opt. Laser Eng.* **27** 321–33
[8] Fu Y, Guo M and Liu H 2012 Determination of instantaneous curvature and twist by digital shearography *Opt. Eng.* **51** 083602
[9] Anderson D J, Valera J D and Jones J D C 1993 Electronic speckle pattern interferometry using diode laser stroboscopic illumination *Meas. Sci. Technol.* **4** 982–7
[10] Atcha H and Tatam R P 1994 Heterodyning of fibre optic electronic speckle pattern interferometers using laser diode wavelength modulation *Meas. Sci. Technol.* **5** 704–9
[11] Sirohi R S 2002 Speckle interferometry *Contemp. Phys.* **43** 161–80
[12] Francis D, Tatam R P and Groves R M 2010 Shearography technology and applications: a review *Meas. Sci. Technol.* **21** 102001
[13] Hung Y Y 1997 Digital shearography versus TV-holography for Non-destructive evaluation *Opt. Laser Eng.* **26** 421–36
[14] Steinchen W, Kupfel G, Mäckel P and Vössing F 1999 Determination of strain distribution by means of digital shearography *Measurement* **26** 79–90
[15] Hung Y Y 1996 Shearography for non-destructive evaluation of composite structures *Opt. Laser Eng.* **24** 161–82
[16] Mihaylova E, Naydenova I, Martin S and Toal V 2004 Electronic speckle pattern shearing interferometer with a photopolymer holographic grating *Appl. Opt.* **43** 2439–42
[17] Hathaway R B, Hovanesian J D and Hung M Y Y 1997 Residual stress evaluation using shearography with large shear displacements *Opt. Laser Eng.* **27** 43–60
[18] Hansen R S 2004 A compact ESPI system for displacement measurements of specular reflecting or optical rough surfaces *Opt. Laser Eng.* **41** 73–80
[19] Creath K 1985 Phase-shifting speckle interferometry *Appl. Opt.* **24** 3053–8
[20] Peng S, Joenathan C and Khorana B M 1992 Quasi-equal-path electronic speckle pattern interferometric system *Opt. Lett.* **17** 1040–2
[21] Olszak A and Tatam R P 1997 The calibration of the path-length imbalance in optical fibre ESPI systems employing source wavelength modulation *Meas. Sci. Technol.* **8** 759–63
[22] Ford H D, Atcha H and Tatam R P 1993 Optical fibre technique for the measurement of small frequency separations: application to surface profile measurement using electronic speckle pattern interferometry *Meas. Sci. Technol.* **4** 601–7
[23] Creath K, Cheng Y-Y and Wyant J C 1985 Contouring aspheric surfaces using two-wavelength phase-shifting interferometry *Opt. Act* **32** 1455–64
[24] Masiyano D, Hodgkinson J and Tatam R P 2008 Use of diffuse reflections in tunable diode laser absorption spectroscopy: implications of laser speckle for gas absorption measurements *Appl. Phys.* B **90** 279–88
[25] Hariharan P, Oreb B F and Eiju T 1987 Digital phase shifting interferometry: a simple error-compensating phase calculation algorithm *Appl. Opt.* **26** 2504–6
[26] Steinchen W, Yang L, Kupfer G and Mäckel P 1998 Non-destructive testing of aerospace composite materials using digital shearography *Proc. Inst. Mech. Eng. G: J. Aerospace Eng.* **212** 21–30
[27] Aebischer H A and Waldner S 1999 A simple and effective method for filtering speckle interferometric phase fringe patterns *Opt. Commun.* **162** 205–10
[28] Herráez M A, Gdeisat M A, Burton D R and Lalor M J 2002 Robust, fast, and effective 2D automatic phase unwrapping algorithm based on image decomposition *Appl. Opt.* **41** 7445–55
[29] www.ljmu.ac.uk/GERI/90207.htm (accessed 11/03/2015).
[30] Schmit J and Hariharan P 2006 Two-wavelength interferometric profilometry with a phase-step error-compensating algorithm *Opt. Eng.* **45** 115602
[31] Kumar U P, Bhaduri B, Kothiyal M P and Krishna Mohan N 2009 Two-wavelength micro-interferometry for 3-D surface profiling *Opt. Laser Eng.* **47** 223–9
[32] Kumar U P, Krishna Mohan N, Kothiyal M P and Asundi A K 2009 Deformation and shape measurement using multiple wavelength microscopic TV holography *Opt. Eng.* **48** 023601